ChemPubSoc Europe

DOI: 10.1002/chem.201503943

CHEMISTRY
A European Journal
Full Paper

Imaging | *Very Important Paper*

VIP A Three-Component Assembly Promoted by Boronic Acids Delivers a Modular Fluorophore Platform (BASHY Dyes)**

Fábio M. F. Santos,[a] João N. Rosa,[a] Nuno R. Candeias,[b] Cátia Parente Carvalho,[c] Ana I. Matos,[a] Ana E. Ventura,[a] Helena F. Florindo,[a] Liana C. Silva,[a] Uwe Pischel,*[c] and Pedro M. P. Gois*[a]

Abstract: The modular assembly of boronic acids with Schiff-base ligands enabled the construction of innovative fluorescent dyes [boronic acid salicylidenehydrazone (BASHY)] with suitable structural and photophysical properties for live cell bioimaging applications. This reaction enabled the straightforward synthesis (yields up to 99%) of structurally diverse and photostable dyes that exhibit a polarity-sensitive green-to-yellow emission with high quantum yields of up to 0.6 in nonpolar environments. These dyes displayed a high brightness (up to 54000 $M^{-1}cm^{-1}$). The promising structural and fluorescence properties of BASHY dyes fostered the preparation of non-cytotoxic, stable, and highly fluorescent poly(lactide-*co*-glycolide) nanoparticles that were effectively internalized by dendritic cells. The dyes were also shown to selectively stain lipid droplets in HeLa cells, without inducing any appreciable cytotoxicity or competing plasma membrane labeling; this confirmed their potential as fluorescent stains.

Introduction

The quest for flexible and modular approaches that enable the construction of electronically tunable and environmentally responsive fluorophore platforms is vital for the development of functional dyes for bioimaging, sensing, and probing applications.[1–5] Highly fluorescent dyes based, for example, on rhodamine,[6,7] fluorescein,[3,8] oxazine,[3] coumarin,[3] cyanine[9,10] or boron dipyrromethene (BODIPY)[11–15] chromophores, have been extensively explored along these lines. In particular, BODIPY derivatives (Scheme 1 A) became the focus of different fields due to a combination of remarkable photophysical properties, which included very high quantum yields, narrow absorption and emission bands, and high molar absorption coefficients.

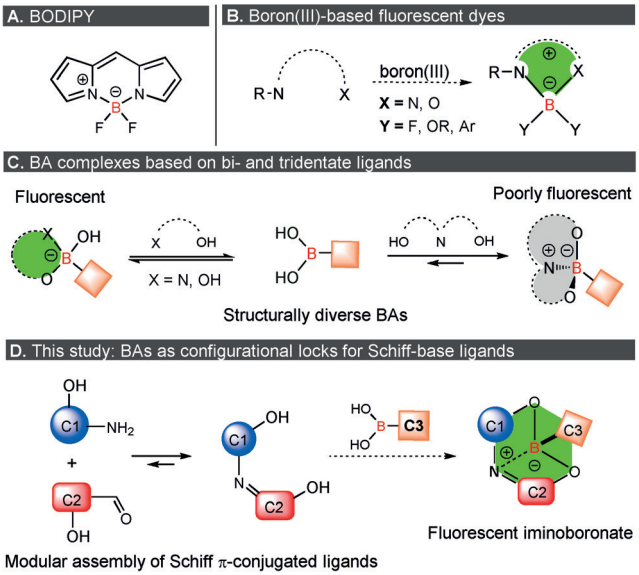

Scheme 1. General structures of A) BODIPY and B) boron-based fluorophores. C) Complexation of boronic acids (BAs) with bi- and tridentate ligands. D) Design of fluorescent dyes with Schiff-base ligands and BAs.

The success of BODIPY dyes triggered burgeoning interest in the engineering of sophisticated fluorescent molecules featuring a central boron(III) atom coordinated to a bidentate ligand, usually with N,N or N,O charged sites, and two anions, typically F^- or Ar^- (Scheme 1 B).[16] Likewise, four-coordinate or-

[a] F. M. F. Santos, Dr. J. N. Rosa, A. I. Matos, A. E. Ventura, Dr. H. F. Florindo, Dr. L. C. Silva, Dr. P. M. P. Gois
Research Institute for Medicines (iMed.ULisboa)
Faculty of Pharmacy, University of Lisbon
Av. Prof. Gama Pinto, 1649-003, Lisbon (Portugal)
E-mail: pedrogois@ff.ulisboa.pt

[b] Dr. N. R. Candeias
Department of Chemistry and Bioengineering
Tampere University of Technology
Korkeakoulunkatu 8, 33101 Tampere (Finland)

[c] C. P. Carvalho, Dr. U. Pischel
CIQSO - Center for Research in Sustainable Chemistry
and Department of Chemistry, University of Huelva
Campus de El Carmen s/n, 21071 Huelva (Spain)
E-mail: uwe.pischel@diq.uhu.es

[**] BASHY = boronic acid salicylidenehydrazone.

Supporting information for this article is available on the WWW under http://dx.doi.org/10.1002/chem.201503943.

ganoboron N,C chelates have been investigated intensively; some of them are highly fluorescent and strongly indicate their suitability for applications in organic light-emitting materials.[17] In many of these architectures, the boron atom assumes an instrumental role because it may improve the stability of the ligand and enhance the planarity of the dye, conjugation, and charge transfer throughout the π system.[16] Therefore, it is rather surprising that widely available and structurally diverse BAs have been generally overlooked as useful conformational blocks for the construction of fluorescent dyes.

The lack of use of BAs may suggest some difficulties in the self-assembled generation of fluorescent molecules based on this function. BAs are known to feature a rich supramolecular chemistry[18–22] and to form fluorescent complexes upon binding with bidentate ligands.[23–26] However, the coordination is reversible and the conjugates often lack the long-term stability required for their application as functional dyes (Scheme 1 C). Differently, BAs generate more stable complexes with tridentate ligands, although these boronates are poorly fluorescent because the central boron atom adopts an out-of-plane tetrahedral geometry (Scheme 1 C).[27]

BAs offer attractive opportunities for the discovery of fluorescent supramolecular architectures, since this function may be used to rigidify unreported structures of tridentate π-conjugated ligands, which can be further tuned, depending on the BA structure. Bearing this in mind, we envisioned that Schiff-base ligands could be used as a platform to build fluorescent boronates, since the modular structure of these ligands can be specifically engineered to accommodate BAs in form of a conformationally stable π-conjugated complex (Scheme 1 D).[28–32] The result of this design effort is a modular fluorophore platform based on boronic acid salicylidenehydrazone (BASHY) complexes.

Results and Discussion

Stepwise molecular development of BASHY dyes

Boronates prepared by using Schiff-base ligands and BAs were used recently by us to prepare new, biologically active, small molecules and to selectively functionalize proteins.[33–37] In the course of these studies,[35] we observed that boronate **1** (Scheme 2) was weakly fluorescent ($\lambda_{fluo}=456$ nm, $\Phi_{fluo}=0.03$; quantitative data in acetonitrile determined in this work). Based on this observation, and with the aim of discovering a modular BA-based molecular platform for the construction of functional fluorescent dyes, boronate **2** was designed (Scheme 2). In comparison to **1**, this compound was predicted to feature a more extended π framework, improved ligand planarity, and greater rigidity; all of these are attributes for the observation of significant and bathochromically shifted fluorescence. Hence, 4-methoxysalicylaldehyde, anthranilic acid, and phenylboronic acid were reacted in ethanol for 18 h at 70 °C. This simple, three-component protocol afforded the desired compound, which was isolated by filtration in high purity and 90% yield. To our disappointment, boronate **2** proved to be only very poorly fluorescent ($\Phi_{fluo}<0.01$), albeit with the predicted bathochromically shifted emission ($\Delta\lambda=42$ nm). Thus, it was anticipated that the installation of a hydrazone bridge between the donor and acceptor components could enhance π conjugation along the main axis of the ligand and contribute to improved fluorescence properties of the dye. To put this idea into practice, 4-methoxysalicylhydrazone (**3**), phenylglyoxylic acid, and phenylboronic acid were reacted in acetonitrile. After heating at 80 °C for 2 h, BASHY complex **5** was isolated in near quantitative yield as a solid of high purity (Scheme 2). Indeed, this dye was significantly more fluorescent than boronates **1** and **2**, and also displayed a further bathochromic shift of the emission band ($\lambda_{fluo}=506$ nm, $\Phi_{fluo}=0.17$; in acetonitrile).

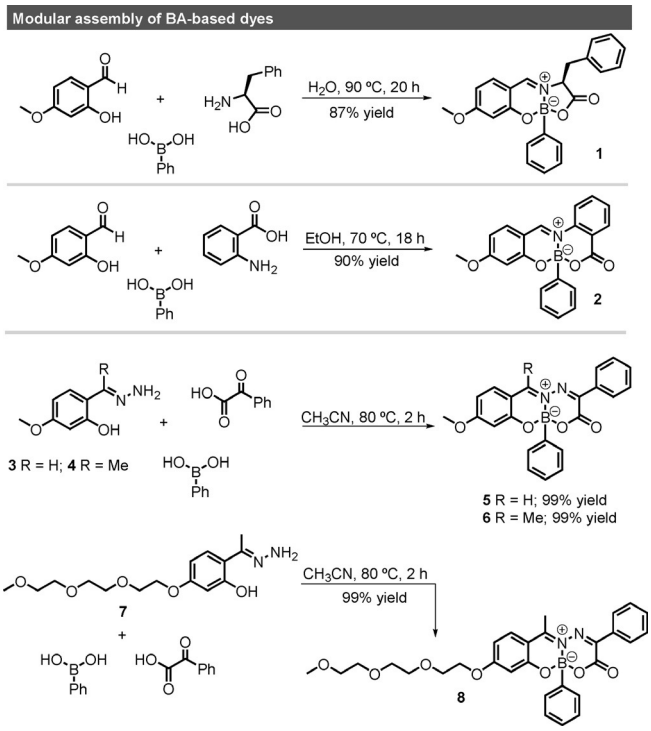

Scheme 2. One pot-assembly of BA-based heterocycles; the yields presented were obtained without any chromatographic purification steps.

Expansion of the scope of BASHY dyes

Encouraged by the previous result, we addressed the synthesis of different BASHY constructs based on the above-described three-component reaction. As shown in Scheme 2, iminoboronate **6** was readily obtained from **4** in 99% yield. Dye **8**, electronically analogous to dye **6**, but featuring a PEG-ylated side chain (PEG = polyethylene glycol), was also efficiently assembled by using this protocol. Interestingly, the addition of the PEG functionality did not impair the photophysical properties of the dye (see below and spectra in the Supporting Information).

The installation of a stronger electron-donating *N*,*N*-diethylamino substituent proved slightly more challenging because the reaction of hydrazine with 4-diethylaminosalicylaldehyde led invariably to the formation of the undesired bis-hydrazone.

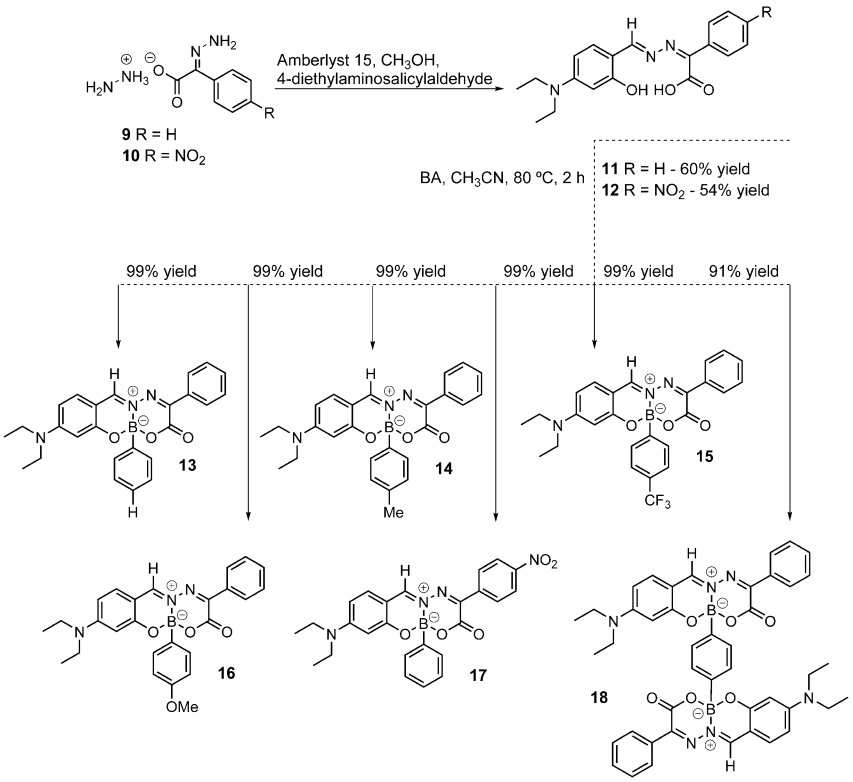

Scheme 3. Synthesis of BA-based heterocycles featuring an *N*,*N*-diethylamino substituent; the yields presented were obtained without any chromatographic purification steps.

Therefore, a new method, involving the formation of hydrazones from phenylglyoxylic acid derivatives (**9** and **10**), was developed to overcome this obstacle (Scheme 3). This procedure enabled the synthesis of ligands **11** and **12**, which were then converted into dyes **13**–**18** in excellent to almost quantitative yields (up to 99%) by simple condensation with the appropriate BA derivative. The simplicity of the method is underpinned by the fact that the dyes are readily obtained in high purity and without the need for additional chromatographic steps.

Photophysical properties of BASHY dyes

Taking the fluorescent nature of the first BASHY dye, **5** (see above), as a starting point, a more systematic investigation of some of the newly prepared dyes was performed. The data are compiled in Table 1 and representative UV/Vis absorption and fluorescence spectra are shown in Figure 1 A.

The instrumental role of the BA component as a conformational block of the essentially nonfluorescent ligand was confirmed in a control experiment with **12**. Upon addition of three equivalents of phenylboronic acid to the ligand (leading to the slow formation of dye **17**), the buildup of the typical fluorescence band (enhancement factor of ca. 150 within 95 h) was observed (see the Supporting Information).

Dye **13**, which featured a strongly electron-donating *N*,*N*-diethylamino group, showed a further bathochromic shift (by ca. 40 nm) in polar solvents, such as acetonitrile ($\lambda_{fluo} = 540$ nm, $\Phi_{fluo} = 0.08$; Figure 1 A), relative to those of methoxy-substituted **5** and **6**. However, in nonpolar solvents, the emission maximum of **13** was displaced hypsochromically ($\lambda_{fluo} = 508$ nm in toluene and 517 nm in chloroform; Figure 1 B and Table 1).

Table 1. Photophysical properties of BASHY dyes in air-equilibrated solution.

	Solvent[a]	λ_{abs} [nm][b]	λ_{fluo} [nm][c]	Φ_{fluo}[d]	τ_{fluo} [ns][e]
1	CH_3CN	363	456	0.03	0.49
2	CH_3CN	401	498	< 0.01	–[f]
5	CH_3CN	420	506	0.17	1.59
6	CH_3CN	415	503	0.16	1.45
8	CH_3CN	415	497	0.15	1.39
8	$CHCl_3$	424	494	0.13	1.07
8	TOL	424	500	0.10	0.86
13	CH_3OH	473	544	< 0.01	–[f]
13	CH_3CN	471	540	0.08	0.43
13	$CHCl_3$	477	517	0.62	2.70
13	TOL	471	508	0.60	2.38
14	CH_3CN	472	540	0.09	0.59
15	CH_3CN	471	542	0.06	0.36
16	CH_3CN	471	540	0.09	0.52
17	CH_3OH	487	592	< 0.01	–[f]
17	CH_3CN	488	632	< 0.01	–[f]
17	$CHCl_3$	496	555	0.48	2.85
17	TOL	489	535	0.55	2.64
18	CH_3CN	463	534	0.06	0.65
18	$CHCl_3$	472	520	0.53	3.47

[a] TOL = toluene. [b] Longest-wavelength absorption maximum. [c] Fluorescence maximum. [d] Fluorescence quantum yield. [e] Fluorescence lifetime. [f] Not determined because of the low emission intensity.

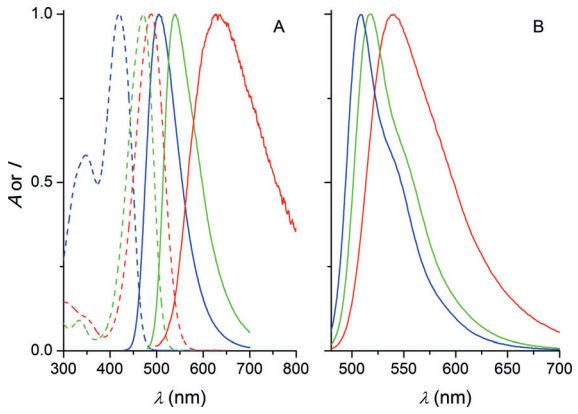

Figure 1. A) UV/Vis absorption (dashed lines) and fluorescence spectra (solid lines) of dyes **5** (blue), **13** (green), and **17** (red) in acetonitrile. B) Fluorescence spectra of **13** in toluene (blue), chloroform (green), and acetonitrile (red).

The substituent effect (**5** versus **13**) on the spectral position of the rather broad emission bands and the solvent effect pinpoint the intramolecular charge-transfer (ICT) character of the dye (see also below).[38] The observed pronounced Stokes shifts (70–80 nm) are another typical feature of ICT fluorophores. This enables their excitation far from the spectral window of emission observation. Accordingly, potential complications in fluorescence microscopy, such as stray-light detection or the reabsorption of emitted photons, are avoided. These problems are often encountered for BODIPY dyes and require alternative photophysical designs, such as energy-transfer cassettes.[13,39] The ICT character of the BASHY dyes was further supported by time-dependent (TD) DFT calculations[40] at the CAM-B3LYP/6-31G** level of theory (see the Supporting Information).

Energetically low-lying ICT states often deactivate through competitive nonradiative channels. This is a direct consequence of the phenomenon known as the energy gap law and explains the relatively low quantum yields of BASHY dyes in polar solvents, which stabilize the ICT state.[38] However, this also means that in nonpolar solvents the fluorescence quantum yields should increase significantly, which indeed was verified by values as high as 0.60–0.62 (Table 1). The emission properties of the BASHY dyes are invariable with the substitution pattern of the phenylboronic acid component, as exemplified for the series of dyes **13**–**16** and **18**. This is an important observation, which enables the electronically innocent modification of the dyes and even the preparation of dimers, such as dye **18**, in which both halves are electronically noncommunicating (see also DFT calculations in the Supporting Information).[29] Hence, dye **18** maintains the fluorescence properties of **13** (see Table 1), but nearly doubles the molar absorption coefficient (60 000 $M^{-1}cm^{-1}$ for **13** versus 103 900 $M^{-1}cm^{-1}$ for **18** in acetonitrile). The exaggeration of the electron-accepting properties of the nitrophenyl substituent at the α-carbonyl position in dye **17** displaced the emission maximum further to $\lambda = 632$ nm in acetonitrile (Figure 1 A), but at the cost of its fluorescent nature ($\Phi_{fluo} < 0.01$). Again, the energy-gap law is behind these observations. As expected for a push–pull dye with strong ICT character, also a strong solvatochromic effect for **17**, an effective hypsochromic shift of the fluorescence emission in nonpolar solvents ($\lambda_{fluo} = 535$ nm in toluene and 555 nm in chloroform; see Table 1 and spectra in Supporting Information) was noted. Again, this was accompanied by fluorescence light-up behavior in nonpolar media ($\Phi_{fluo} = 0.55$ and 0.48 in toluene and chloroform, respectively; see Table 1).

The brightness ($\varepsilon \times \Phi_{fluo}$) of dyes **13**, **17**, and **18** in nonpolar environments was determined for the excitation at their absorption maxima, which serendipitously in the case of the *N*,*N*-diethylamino-substituted dyes **13**–**18** matched quite well with the output lines of the Ar^+ laser ($\lambda = 488$, 476 nm), frequently used in confocal fluorescence microscopy setups. Brightness values as high as 37 000, 28 000, and 54 000 $M^{-1}cm^{-1}$ were obtained for **13**, **17**, and **18**, respectively, in nonpolar media (i.e., chloroform). These values are comparable to those of other well-performing fluorescent dyes, for example, cyanine dyes (Cy3, 18 000 $M^{-1}cm^{-1}$), carbofluorescein (67 000 $M^{-1}cm^{-1}$), tetramethylrhodamines (35 000 $M^{-1}cm^{-1}$), or phenoxazine dyes (resorufin, 41 000 $M^{-1}cm^{-1}$).[3] The high brightness and environmentally sensitive fluorescence render BASHY dyes promising candidates for applications in bioimaging. Of particular interest is their use as stains for nonpolar, hydrophobic intracellular environments, such as lipid droplets (see below),[41] as an interesting alternative for commonly employed Nile red.[42,43]

The photostability is another issue that was evaluated. As shown in Table 2, dyes **13**, **17**, and **18** are very photostable in acetonitrile and chloroform, with less than 15% decomposition (as rated by the intensity of the fluorescence signal) after irradiation for 3 h with a 150 W xenon lamp and a $\lambda = 455$ nm cutoff filter (see also the Supporting Information). As observed for other dyes, the excited ICT state serves as an energy sink, thereby protecting the molecules from unwanted photodecompositon.[44]

Table 2. Photostability of selected BASHY dyes in air-equilibrated solution.

	Solvent	$I_{fluo}/I_0 \times 100\%$[a]
13	CH_3CN	90
	$CHCl_3$	90
17	CH_3CN	–[b]
	$CHCl_3$	96
18	CH_3CN	92
	$CHCl_3$	87
Nile red	CH_3CN	81
	$CHCl_3$	93

[a] After irradiation for 3 h with a 150 W xenon lamp equipped with a $\lambda = 455$ nm cutoff filter; followed by fluorescence. [b] Not determined because of low fluorescence; the UV/Vis absorption spectrum indicates no photodecomposition.

Encapsulation in polymeric nanoparticles (NPs)

Having established the molecular diversity and photophysical properties of BASHY dyes, we explored their use in bioimaging

applications. In the first step, we were interested in their entrapment in polymeric NPs, which have recently received considerable attention as promising drug-delivery vehicles.[45,46] In this context, fluorophore-labeled NPs are highly appreciated tools to evaluate the biophysical properties of NPs at the cellular level in confocal microscopy studies. Such conjugates potentially foster a better understanding of the recognition and uptake mechanisms by target cells,[47,48] and also provide a means to evaluate undesired side effects, such as bioaccumulation, cytotoxicity, and the triggering of unwanted cellular responses.[49–51] Furthermore, encapsulation in NPs provides additional protection of the dyes from slow hydrolytic degradation, which was observed for the free dyes (e.g., $t_{1/2}$ ca. 3 h for **6** at pH 4.5). However, in toluene, the dyes (e.g., **13**) show practically no degradation over 12 h. A similar stability level is expected for the nonpolar environment of NPs, such as the herein explored poly(lactide-*co*-glycolide) (PLGA) NPs.[52,53]

The application of the double emulsion–solvent evaporation method resulted in fluorescent PLGA-based NPs (Figure 2B) with quantitative entrapment of dyes **13** and **17**. Their physicochemical properties (see also Supporting Information) are identical to those of unlabeled NPs or conjugates with standard fluorophores, such as coumarin-6. The mean diameter ((185 ± 7) nm for unloaded PLGA NPs versus (182 ± 3) to (189 ± 8) nm for dye-labeled NPs), narrow particle size distribution (polydispersity index (PdI); 0.054 ± 0.018 for unloaded NPs versus 0.050 ± 0.022 to 0.088 ± 0.034 for dye-labeled NPs), and a zeta potential close to neutrality (ranging from (−1.64 ± 0.39) to (−3.51 ± 0.36) mV at pH 7.4) were maintained upon dye encapsulation. On one hand, it was observed that the BASHY dyes were not released in vitro from the nanoparticulate polymer matrix in RPMI (Roswell Park Memorial Institute) cell culture media over a period of 24 h at 37 °C (see the Supporting Information). On the other hand, undesired dye leaching was clearly observed for the coumarin-labeled PLGA NPs under the same experimental conditions.

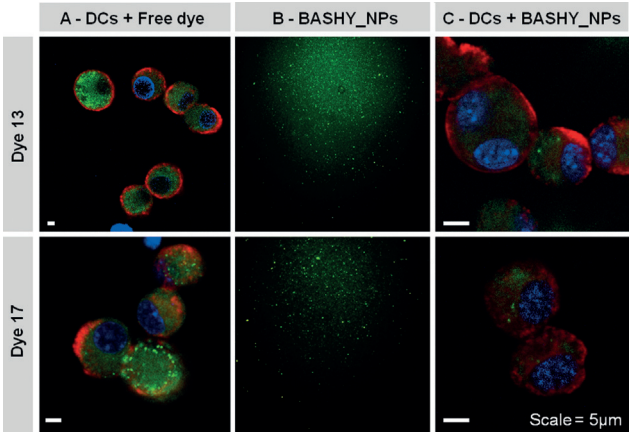

Figure 2. A) Confocal microscopy images obtained after incubation of immature bone-marrow-derived murine dendritic cells (DCs) with BASHY dyes (2.5 μg mL^{-1}; green) and C) BASHY-labeled PLGA NPs (0.5 mg mL^{-1}; green), for 10 min and 18 h, respectively. The plasma membrane (PM) was stained with WGA-Alexa Fluor 633 (5 μg mL^{-1}; red), whereas Hoechst 33342 (1 μg mL^{-1}) was used for nucleus labeling (blue), after 10 min of incubation. B) Fluorescence microscopy images of BASHY-labeled PLGA NPs.

In accordance with the polarity-dependent fluorescence of the dyes, the nonpolar microenvironment provided by the polymer matrix makes these NPs rather brightly fluorescent. These dye-labeled NPs have lost their environmental polarity sensitivity, but can now be explored as inherently fluorescent tags in confocal microscopy. DCs were selected as biological models. This choice was motivated by their currently unfolding potential in the development of prophylactic and therapeutic vaccines.[54] As shown in Figure 2C, BASHY-labeled NPs were successfully taken up by immature bone-marrow-derived murine DCs after 18 h of incubation time. The internalization process for both dye-labeled NPs was unequivocally demonstrated by Z-stack confocal microscopy images, which clearly provided evidence of intracellular localization (Figure 2C) and excluded external adsorption onto the PM. The microscopic images of the DCs incubated with the unsupported dyes showed qualitatively the same fluorescence patterns (Figure 2A). Importantly, the BASHY-labeled NPs were shown to exhibit low cytotoxicity, reaching high levels of cell viability (> 90 %), even 24 h after incubation (Figure 3A).

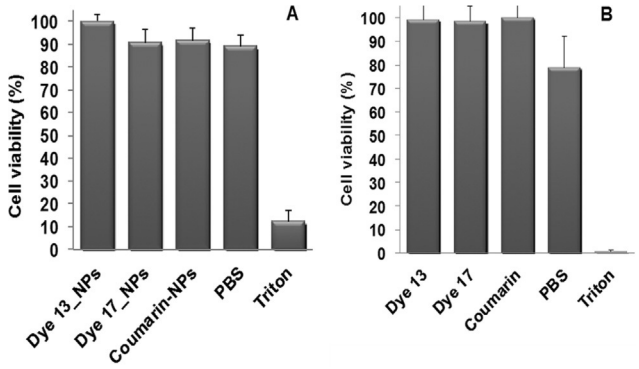

Figure 3. Cell viability determined by AlamarBlue assay 24 h after incubation of A) DCs (JAW SII, ATCC CRL-11904TM) with 500 μg mL^{-1} of dye-labeled NPs (**13**, **17** or coumarin-6) or B) HeLa cells with 5 μg mL^{-1} of dye (**13**, **17** or coumarin-6); mean ± standard deviation (SD); $n = 6$. Phosphate-buffered saline (PBS) and Triton were used as controls.

Bioimaging of lipid droplets

Considering the hydrophobic asymmetric 3D structure of the dyes and their fluorescence in nonpolar environments, it was envisioned that these compounds could be used as selective lysochromic stains for lipid droplets. These targets are highly dynamic lipid reservoirs with implications in the regulation of intracellular lipid storage and metabolism.[41] With this objective in mind, the labeling of HeLa cells with BASHY dyes **13** and **17** was performed (Figure 4). To contrast localization of the dyes, PM-selective WGA-Alexa Fluor 633 and DNA-binding Hoechst 33342 were employed in a costaining protocol (Figure 4A). Under the chosen experimental conditions, the viability of the HeLa cells was high and unaffected by the presence of the BASHY dyes (Figure 3B). As observed for the DCs (Fig-

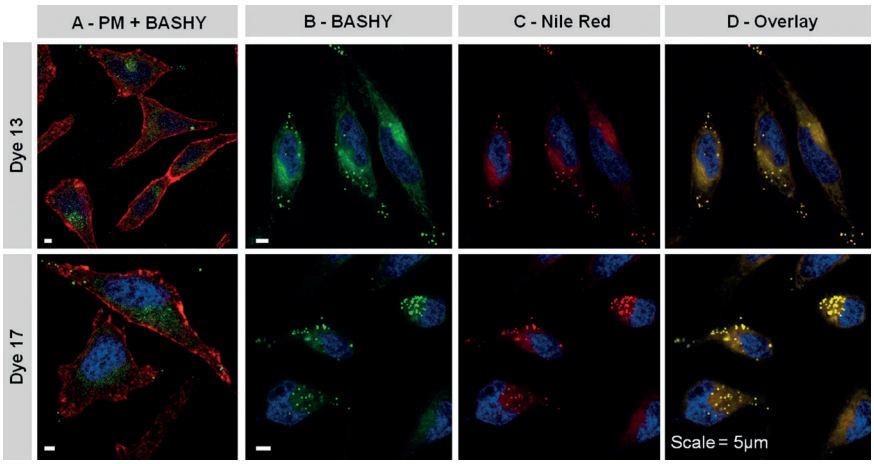

Figure 4. Confocal fluorescence microscopy images of HeLa cells. A) and B) Labeled with BASHY dyes **13** or **17** (2.5 μg mL^{-1}; green), and A) additionally with WGA-Alexa Fluor 633 (5 μg mL^{-1}; red) as the PM stain, after 10 min of incubation. C) Labeled with Nile red (1 μg mL^{-1}) for lipid droplet staining (red), during 10 min. D) Overlay images of B) and C). Hoechst 33342 (1 μg mL^{-1}) was used for nucleus labeling (blue) in all images.

ure 2A), both BASHY dyes were readily internalized by HeLa cells and accumulated at intracellular structures of variable sizes and cellular distribution (Figure 4). Remarkably, the BASHY dyes did not partition into structures that displayed a tighter lipid packing, such as the PM.[55] Hence, these dyes could be used to differentiate between membrane regions with variable packing properties.

To confirm whether BASHY dyes did indeed selectively label lipid droplets, they were used together with the archetypal lipid droplet stain Nile red[42,43] in dual color experiments (Figure 4C and D). The colocalization analysis and determination of Pearson's correlation coefficient ($R_r = 0.85$ and 0.94 for colocalization between Nile red and dyes **13** and **17**, respectively) provided compelling evidence for selective lipid droplet staining by BASHY dyes; this underpins their potential for live-cell bioimaging applications.

Conclusion

For the first time, it was shown that BAs are valuable building blocks for the multicomponent assembly of a functionally and structurally versatile fluorescent dye platform. The simple synthetic protocol afforded the dyes in high yields without the need for laborious chromatographic steps. The modularity of the synthetic approach allows the integration of virtually any functionality. The resulting photostable fluorescent dyes, conveniently modified with electron-donating substituents, show polarity-sensitive green-to-yellow emission with quantum yields of up to 0.6 in nonpolar environments. The brightness of these new dyes approaches that of widely commercialized fluorescence imaging standards, such as cyanine dyes or rhodamines. These new dyes were successfully used as staining agents for bioimaging applications. They were efficiently entrapped in PLGA NPs and these stable conjugates were shown to be readily internalized by DCs, without showing any negative effect on cell viability. The unsupported dyes were demonstrated to be selective staining agents of lipid droplets in HeLa cells, and matched the performance of the archetypal Nile red dye.

The development of new live-cell imaging methodologies is vital to foster new research in cell biology. Therefore, we envision that this BASHY platform, featuring dyes with remarkable photophysical properties, low toxicity, amenability for NP labeling, and selectivity towards subcellular structures, will emerge as a powerful tool for the tailored design of fluorescent dyes for advanced bioimaging applications.

Experimental Section

General procedures for the synthesis of BASHY dyes

Multicomponent construction of BASHY dyes 5, 6, and 8: Stoichiometric amounts (0.1 mmol) of the corresponding salicylhydrazone derivative, phenylglyoxylic acid, and phenylboronic acid were dissolved in acetonitrile (1 mL), and the reaction mixture was then stirred at 80 °C for 2 h in a round-bottomed flask. The volatile compounds were evaporated under reduced pressure and the BASHY dyes were readily obtained as solids with high purity in near quantitative yield (99%). Characterization data can be found in the Supporting Information.

Ligand-based construction of the BASHY dyes 13–18: The corresponding ligand (0.1 mmol for **13**–**17** and 0.2 mmol for **18**) and phenylboronic acid derivative (0.1 mmol) were dissolved in acetonitrile (1 mL), and the reaction mixture was heated at 80 °C for 2 h in a round-bottomed flask. Then the volatile compounds were evaporated under reduced pressure to yield the corresponding BASHY dye with high purity in near quantitative yield. In some cases, the obtained solids were washed with cold methanol (0.5 mL) to remove very minor impurities. Characterization data can be found in the Supporting Information.

Details on the experimental procedures corresponding to the photophysical characterization, NP preparation, cell experiments, and confocal microscopy are described in the Supporting Information.

Acknowledgements

We acknowledge financial support from the Fundação para a Ciência e a Tecnologia (FCT) Portugal (grants SFRH/BD/81628/2011, SFRH/BD/94779/2013, PTDC/QUI-QUI/118315/2010, PTDC/SAUFAR/119389/2010, PTDC/BBB-BQB/0506/2012; L.C.S. and P.M.P.G. are FCT Investigators; iMed.ULisboa grant UID/DTP/04138/2013), the Ministerio de Economía y Competitividad, Madrid, Spain (grant CTQ2014-54729-C2-1-P), and the Junta de Andalucía (grant P12-FQM-2140). N.R.C. is grateful to the CSC-IT Center for Science Ltd. for the allocation of computational resources.

Keywords: boron · charge transfer · dyes/pigments · fluorescence · imaging

[1] A. P. de Silva, H. Q. N. Gunaratne, T. Gunnlaugsson, A. J. M. Huxley, C. P. McCoy, J. T. Rademacher, T. E. Rice, *Chem. Rev.* **1997**, *97*, 1515.
[2] R. N. Dsouza, U. Pischel, W. M. Nau, *Chem. Rev.* **2011**, *111*, 7941.
[3] L. D. Lavis, R. T. Raines, *ACS Chem. Biol.* **2014**, *9*, 855.
[4] X. Li, X. Gao, W. Shi, H. Ma, *Chem. Rev.* **2014**, *114*, 590.
[5] J. Yin, Y. Hu, J. Yoon, *Chem. Soc. Rev.* **2015**, *44*, 4619.
[6] M. Beija, C. A. M. Afonso, J. M. G. Martinho, *Chem. Soc. Rev.* **2009**, *38*, 2410.
[7] J. B. Grimm, B. P. English, J. Chen, J. P. Slaughter, Z. Zhang, A. Revyakin, R. Patel, J. J. Macklin, D. Normanno, R. H. Singer, T. Lionnet, L. D. Lavis, *Nat. Methods* **2015**, *12*, 244.
[8] Y. Kushida, T. Nagano, K. Hanaoka, *Analyst* **2015**, *140*, 685.
[9] K. Kiyose, H. Kojima, T. Nagano, *Chem. Asian J.* **2008**, *3*, 506.
[10] E. M. S. Stennett, M. A. Ciuba, M. Levitus, *Chem. Soc. Rev.* **2014**, *43*, 1057.
[11] A. Coskun, E. U. Akkaya, *J. Am. Chem. Soc.* **2006**, *128*, 14474.
[12] A. Loudet, K. Burgess, *Chem. Rev.* **2007**, *107*, 4891.
[13] G. Ulrich, R. Ziessel, A. Harriman, *Angew. Chem. Int. Ed.* **2008**, *47*, 1184; *Angew. Chem.* **2008**, *120*, 1202.
[14] S. Ozlem, E. U. Akkaya, *J. Am. Chem. Soc.* **2009**, *131*, 48.
[15] S. Kolemen, M. Işık, G. M. Kim, D. Kim, H. Geng, M. Buyuktemiz, T. Karatas, X.-F. Zhang, Y. Dede, J. Yoon, E. U. Akkaya, *Angew. Chem. Int. Ed.* **2015**, *54*, 5340; *Angew. Chem.* **2015**, *127*, 5430.
[16] D. Frath, J. Massue, G. Ulrich, R. Ziessel, *Angew. Chem. Int. Ed.* **2014**, *53*, 2290; *Angew. Chem.* **2014**, *126*, 2322.
[17] Y.-L. Rao, S. Wang, *Inorg. Chem.* **2011**, *50*, 12263.
[18] N. Y. Edwards, T. W. Sager, J. T. McDevitt, E. V. Anslyn, *J. Am. Chem. Soc.* **2007**, *129*, 13575.
[19] N. Iwasawa, H. Takahagi, *J. Am. Chem. Soc.* **2007**, *129*, 7754.
[20] A. Schiller, R. A. Wessling, B. Singaram, *Angew. Chem. Int. Ed.* **2007**, *46*, 6457; *Angew. Chem.* **2007**, *119*, 6577.
[21] N. Christinat, R. Scopelliti, K. Severin, *Angew. Chem. Int. Ed.* **2008**, *47*, 1848; *Angew. Chem.* **2008**, *120*, 1874.
[22] Y. Kubo, R. Nishiyabu, T. D. James, *Chem. Commun.* **2015**, *51*, 2005.
[23] Y. Kubo, A. Kobayashi, T. Ishida, Y. Misawa, T. D. James, *Chem. Commun.* **2005**, 2846.
[24] T. E. Barder, S. L. Buchwald, *Org. Lett.* **2007**, *9*, 137.
[25] J. W. Tomsho, S. J. Benkovic, *J. Org. Chem.* **2012**, *77*, 2098.
[26] M. R. Aronoff, B. VanVeller, R. T. Raines, *Org. Lett.* **2013**, *15*, 5382.
[27] R. Chan-Navarro, V. M. Jiménez-Pérez, B. M. Muñoz-Flores, H. V. R. Dias, I. Moggio, E. Arias, G. Ramos-Ortíz, R. Santillan, C. García, M. E. Ochoa, M. Yousufuddin, N. Waksman, *Dyes Pigm.* **2013**, *99*, 1036.
[28] H. Reyes, B. M. Muñoz, N. Farfán, R. Santillan, S. Rojas-Lima, P. G. Lacroix, K. Nakatani, *J. Mater. Chem.* **2002**, *12*, 2898.
[29] J. F. Lamère, P. G. Lacroix, N. Farfán, J. M. Rivera, R. Santillan, K. Nakatani, *J. Mater. Chem.* **2006**, *16*, 2913.
[30] B. M. Muñoz, R. Santillan, M. Rodríguez, J. M. Méndez, M. Romero, N. Farfán, P. G. Lacroix, K. Nakatani, G. Ramos-Ortíz, J. L. Maldonado, *J. Organomet. Chem.* **2008**, *693*, 1321.
[31] M. Rodríguez, G. Ramos-Ortíz, M. I. Alcalá-Salas, J. L. Maldonado, K. A. López-Varela, Y. López, O. Domínguez, M. A. Meneses-Nava, O. Barbosa-García, R. Santillan, N. Farfán, *Dyes Pigm.* **2010**, *87*, 76.
[32] T. Flagstad, M. T. Petersen, T. E. Nielsen, *Angew. Chem. Int. Ed.* **2015**, *54*, 8395; *Angew. Chem.* **2015**, *127*, 8515.
[33] P. M. S. D. Cal, J. B. Vicente, E. Pires, A. V. Coelho, L. F. Veiros, C. Cordeiro, P. M. P. Gois, *J. Am. Chem. Soc.* **2012**, *134*, 10299.
[34] F. Montalbano, N. R. Candeias, L. F. Veiros, V. André, M. T. Duarte, M. R. Bronze, R. Moreira, P. M. P. Gois, *Org. Lett.* **2012**, *14*, 988.
[35] F. Montalbano, P. M. S. D. Cal, M. A. B. R. Carvalho, L. M. Gonçalves, S. D. Lucas, R. C. Guedes, L. F. Veiros, R. Moreira, P. M. P. Gois, *Org. Biomol. Chem.* **2013**, *11*, 4465.
[36] P. M. S. D. Cal, R. F. M. Frade, V. Chudasama, C. Cordeiro, S. Caddick, P. M. P. Gois, *Chem. Commun.* **2014**, *50*, 5261.
[37] P. M. S. D. Cal, R. F. M. Frade, C. Cordeiro, P. M. P. Gois, *Chem. Eur. J.* **2015**, *21*, 8182.
[38] V. F. Pais, H. S. El-Sheshtawy, R. Fernández, J. M. Lassaletta, A. Ros, U. Pischel, *Chem. Eur. J.* **2013**, *19*, 6650.
[39] J. Fan, M. Hu, P. Zhan, X. Peng, *Chem. Soc. Rev.* **2013**, *42*, 29.
[40] M. E. Casida in *Recent Advances in Density Functional Methods, Vol. 1* (Ed.: D. P. Chong), World Scientific, Singapore, **1995**, pp. 155.
[41] A. R. Thiam, R. V. Farese Jr. , T. C. Walther, *Nat. Rev. Mol. Cell Biol.* **2013**, *14*, 775.
[42] P. Greenspan, S. D. Fowler, *J. Lipid Res.* **1985**, *26*, 781.
[43] D. L. Sackett, J. Wolff, *Anal. Biochem.* **1987**, *167*, 228.
[44] V. F. Pais, M. M. Alcaide, R. Rodríguez-López, D. Collado, F. Nájera, E. Pérez-Inestrosa, E. Álvarez, J. M. Lassaletta, R. Fernández, A. Ros, U. Pischel, *Chem. Eur. J.* **2015**, *21*, 15369.
[45] R. Duncan, R. Gaspar, *Mol. Pharm.* **2011**, *8*, 2101.
[46] C. J. Cheng, G. T. Tietjen, J. K. Saucier-Sawyer, W. M. Saltzman, *Nat. Rev. Drug Discovery* **2015**, *14*, 239.
[47] L. Treuel, X. Jiang, G. U. Nienhaus, *J. R. Soc. Interface* **2013**, *10*, 20120939.
[48] I. M. Adjei, B. Sharma, V. Labhasetwar, *Adv. Exp. Med. Biol.* **2014**, *811*, 73.
[49] C. Peetla, S. Vijayaraghavalu, V. Labhasetwar, *Adv. Drug Delivery Rev.* **2013**, *65*, 1686.
[50] S. Tenzer, D. Docter, J. Kuharev, A. Musyanovych, V. Fetz, R. Hecht, F. Schlenk, D. Fischer, K. Kiouptsi, C. Reinhardt, K. Landfester, H. Schild, M. Maskos, S. K. Knauer, R. H. Stauber, *Nat. Nanotechnol.* **2013**, *8*, 772.
[51] A. Hafner, J. Lovrić, G. P. Lakoš, I. Pepić, *Int. J. Nanomed.* **2014**, *9*, 1005.
[52] F. Danhier, E. Ansorena, J. M. Silva, R. Coco, A. Le Breton, V. Préat, *J. Controlled Release* **2012**, *161*, 505.
[53] J. M. Silva, M. Videira, R. Gaspar, V. Préat, H. F. Florindo, *J. Controlled Release* **2013**, *168*, 179.
[54] K. Palucka, J. Banchereau, *Nat. Rev. Cancer* **2012**, *12*, 265.
[55] D. M. Owen, C. Rentero, A. Magenau, A. Abu-Siniyeh, K. Gaus, *Nat. Protoc.* **2011**, *7*, 24.

Received: October 1, 2015
Published online on December 22, 2015

